

Gold Dithiocarbamate Derivatives as Potential Antineoplastic Agents: Design, Spectroscopic Properties, and in Vitro Antitumor Activity

Luca Ronconi,[†] Lorena Giovagnini,[†] Christine Marzano,[‡] Frazia Bettio,[‡] Rodolfo Graziani,[†] Giuseppe Pilloni,[†] and Dolores Fregona^{*†}

Department of Chemical Sciences, University of Padua, via Marzolo 1, 35131 Padua, Italy, and Department of Pharmaceutical Sciences, University of Padua, via Marzolo 5, 35131, Padua, Italy

Received December 10, 2004

At present, cisplatin (*cis*-diamminodichloroplatinum(II)) is one of the most largely employed anticancer drugs as it is effective in the treatment of 70–90% of testicular and, in combination with other drugs, of ovarian, small cell lung, bladder, brain, and breast tumors. Anyway, despite its high effectiveness, it exhibits some clinical problems related to its use in the curative therapy, such as a severe normal tissue toxicity (in particular, nephrotoxicity) and the frequent occurrence of initial and acquired resistance to the treatment. To obtain compounds with superior chemotherapeutic index in terms of increased bioavailability, higher cytotoxicity, and lower side effects than cisplatin, we report here on some gold(I) and gold(III) complexes with dithiocarbamate ligands (DMDT = *N,N*-dimethyldithiocarbamate; DMDTM = *S*-methyl-*N,N*-dimethyldithiocarbamate; ESDT = ethylsarcosinedithiocarbamate), which have been synthesized, purified, and characterized by means of elemental analyses, conductivity measurements, mono- and bidimensional NMR, FT-IR, and UV–vis spectroscopy, and thermal analyses. Moreover, the electrochemical properties of the designed compounds have been studied through cyclic voltammetry. All the synthesized gold complexes have been tested for their in vitro cytotoxic activity. Remarkably, most of them, in particular gold(III) derivatives of *N,N*-dimethyldithiocarbamate and ethylsarcosinedithiocarbamate, have been proved to be much more cytotoxic in vitro than cisplatin, with IC₅₀ values about 1- to 4-fold lower than that of the reference drug, even toward human tumor cell lines intrinsically resistant to cisplatin itself. Moreover, they appeared to be much more cytotoxic also on the cisplatin-resistant cell lines, with activity levels comparable to those on the corresponding cisplatin-sensitive cell lines, ruling out the occurrence of cross-resistance phenomena and supporting the hypothesis of a different antitumor activity mechanism of action.

Introduction

The high effectiveness of cisplatin in the treatment of several types of tumors is severely hindered by some clinical problems related to its use in the curative therapy, such as a severe normal tissues toxicity and the frequent occurrence of initial and acquired resistance to the treatment. The most important adverse side effect is nephrotoxicity correlated to platinum binding and inactivation of renal thiol-containing enzymes.^{1,2} Anyway, the success of cisplatin in anticancer chemotherapy has raised great interest in the study of metal

complexes to be used as antitumor agents, instigating the ongoing investigation of alternative metal-based drugs.^{3–6}

In this context, attention has been directed toward gold compounds owing to their antiarthritic activity.⁷ In fact, the investigation of the efficacy of anticancer drugs, e.g. 6-mer-

* Author to whom correspondence should be addressed. E-mail: dolores.fregona@unipd.it. Phone: +39-049-8275159. Fax: +39-02-700500560.

[†] Department of Chemical Sciences.

[‡] Department of Pharmaceutical Sciences.

(1) Lippert, B. *Cisplatin: Chemistry and Biochemistry of a Leading Anticancer Drug*; Wiley-VCH: Zurich, 1999.

(2) Dorr, R. T. A review of the modulation of cisplatin toxicities by chemoprotectants. In *Platinum and Other Metal Coordination Compounds in Cancer Chemotherapy 2*; Pinedo, H. M., Schornagel, J. H., Eds.; Plenum Press: New York, 1996; pp 131–154.

(3) Keppler, B. K.; Vogel, E. A. Overview of tumor-inhibiting non-platinum compounds. In *Platinum and Other Metal Coordination Compounds in Cancer Chemotherapy 2*; Pinedo, H. M., Schornagel, J. H., Eds.; Plenum Press: New York, 1996; pp 253–268.

(4) Farrell, N. Transition metal complexes as drugs and chemotherapeutic agents. In *Catalysis by Metal Complexes*; James, B. R., van Leeuwen, P. W. N. M., Eds.; Kluwer Academic Publishers: Dordrecht, The Netherlands, 1989; Vol. 11, pp 44–46.

(5) Allardyce, C. S.; Dyson, P. J. *Platinum Met. Rev.* **2001**, *45*, 62–69.

(6) Guo, Z.; Sadler, P. J. *Angew. Chem., Int. Ed.* **1999**, *38*, 1512–1531.

(7) Best, S. L.; Sadler, P. J. *Gold Bull.* **1996**, *29*, 87–93.

captropurine and cyclophosphamide, in the treatment of rheumatoid arthritis arose from their known immunosuppressive and antiinflammatory actions, and this work established a connection, at least in principle, between the two therapies.⁸ Many investigations have been performed onto the antitumor activity of (phosphine)gold(I) thiolates, such as the well-known antiarthritic drug Auranofin, and most of them have been shown to have useful antitumor activity in vitro but, unfortunately, very limited effectiveness in vivo.⁹

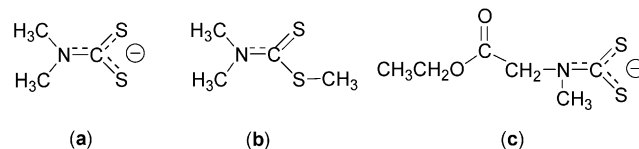
There are, of course, other motivations for the study of the antitumor activity of gold compounds. A commonly cited reason relates to the fact that gold in the +3 oxidation state is isoelectronic with platinum(II), and tetracoordinate gold(III) complexes are found in square-planar geometries¹⁰ resembling, in this regard, the situation found for cisplatin itself. Surprisingly, despite the strict similarity, little literature data exist on the use of gold(III) complexes as anticancer agents;^{11–13} the paucity of data on gold(III) complexes probably derives from their high redox potential and relatively poor stability, which make their use rather problematic under physiological conditions.

Screening for cytotoxicity/antitumor activity of gold(III) compounds dates back to the mid-1970s, but renewed interest is evident as judged from the number of recent papers on the subject. For example, four complexes, namely trichloro-(2-pyridylmethanol)gold(III), dichloro(2-pyridylmethanol)gold(III), dichloro(*N*-methylsalicylaldimine)gold(III), and dichloro(*N*-ethylsalicylaldimine)gold(III), have displayed an interesting cytotoxicity level toward a series of established human tumor cell lines tested and only minimal cross-resistance with cisplatin has been observed.¹⁴ Relevant cytotoxic effects toward a panel of established human cell lines, either cisplatin-sensitive or -resistant, have been also reported for some gold(III) complexes with multidentate ligands (that is, 1,2-ethylenediamine, diethylenetriamine, 1,4,8,11-tetraazacyclotetradecane, terpyridine, phenanthroline, and bipyridyl) allowing further investigation, such as solution chemistry and DNA binding properties.^{15,16}

To obtain compounds with superior chemotherapeutic index in terms of increased bioavailability, higher cytotoxicity, and lower side effects than cisplatin, we report here on some gold(I) and gold(III) dithiocarbamate derivatives which have been synthesized, purified, and characterized by means of elemental analyses, conductivity measurements,

Chart 1. Dithiocarbamate Ligands Used in This Work:

N,N-Dimethyldithiocarbamate (DMDT) (a);
S-Methyl-*N,N*-dimethyldithiocarbamate (DMDTM) (b);
 Ethylsarcosinedithiocarbamate (ESDT) (c)



mono- and bidimensional NMR, FT-IR, and UV-vis spectroscopy, and thermogravimetric analysis. Moreover, the inherent electrochemical properties of the designed compounds have been studied through cyclic voltammetry.

The choice of dithiocarbamate ligands (Chart 1) is not accidental; in fact, dithiocarbamates are still being evaluated for their efficacy as inhibitors of cisplatin-induced nephrotoxicity without decreasing its antitumor activity.^{17–19} Recently, we have reported on a new class of platinum(II) and palladium(II) complexes containing some of these dithiocarbamate ligands and various amines (pyridine, *n*-propylamine, cyclobutylamine, and ethylenediamine) and, in most cases, their cytotoxic activity was greater than cisplatin,^{20,21} moreover, they also showed no cross-resistance with cisplatin and very low in vitro and in vivo nephrotoxicity levels in comparison to the reference drug.²²

The here discussed gold(III) complexes have been selected in such way to reproduce very closely the main features of cisplatin; in fact, all of them exhibit an almost square-planar geometry and contain, at least, two *cis*-gold(III)-halogen bonds that may undergo easy hydrolysis, the remaining coordination positions being occupied by an anionic bidentate or a neutral monodentate dithiocarbamate ligand. Gold(I) analogues of ESDT and DMDTM have been also synthesized for comparison purpose.

After completion of the chemical characterization, all the synthesized gold complexes have been tested for their in vitro cytotoxic activity toward a panel of human tumor cell lines. Remarkably, most of them, in particular gold(III) derivatives of *N,N*-dimethyldithiocarbamate and ethylsarcosinedithiocarbamate, have shown to be 1- to 4-fold more cytotoxic than cisplatin and to be able to overcome to a large extent both intrinsic and acquired resistance to cisplatin itself.

Experimental Section

General Methods. Sodium *N,N*-dimethyldithiocarbamate hydrate, ethylsarcosinehydrochloride, carbon disulfide, ethyl 2-hydroxyethyl sulfide, (Aldrich), methyl iodide (Carlo Erba), and

- (8) Ward, J. R. *Am. J. Med.* **1988**, *85*, 39–44.
 (9) Mirabelli, C. K.; Johnson, R. K.; Sung, C. M.; Faucette, L.; Muirhead, K.; Crooke, S. T. *Cancer Res.* **1985**, *4*, 32–39.
 (10) Puddephat, R. J. *The Chemistry of Gold*; Elsevier: Amsterdam, 1978.
 (11) Tiekink, E. R. T. *Crit. Rev. Oncol. Hematol.* **2002**, *42*, 225–248.
 (12) Dhuhghail, O. M. N.; Sadler, P. J. Gold complexes in cancer chemotherapy. In *Metal Complexes in Cancer Chemotherapy*; Keppler, B. K., Ed.; VCH: Weinheim, Germany, 1993; pp 221–248.
 (13) Sadler, P. J.; Sue, R. E. *Met.-Based Drugs* **1994**, *2–3*, 107–144.
 (14) Calamai, P.; Carotti, S.; Guerri, A.; Mazzei, T.; Messori, L.; Mini, E.; Orioli, P.; Speroni, G. P. *Anti-Cancer Drug Des.* **1998**, *13*, 67–80.
 (15) Messori, L.; Abbate, F.; Marcon, G.; Orioli, P.; Fontani, M.; Mini, E.; Mazzei, T.; Carotti, S.; O'Connell, T.; Zanello, P. *J. Med. Chem.* **2000**, *43*, 3541–3548.
 (16) Marcon, G.; Carotti, S.; Coronello, M.; Messori, L.; Mini, E.; Orioli, P.; Mazzei, T.; Cinellu, M. A.; Minghetti, G. *J. Med. Chem.* **2002**, *45*, 1672–1677.

- (17) Huang, H.; Zhu, L.; Reid, B. R.; Drobny, G. P.; Hopkins, P. B. *Science* **1995**, *270*, 1842–1845.
 (18) Bodenner, D. L.; Dedon, P. C.; Keng, P. C.; Borch, R. F. *Cancer Res.* **1986**, *46*, 2745–2750.
 (19) Borch, R. F.; Dedon, P. C.; Gringeri, A.; Montine, T. J. Inhibition of platinum drug toxicity by diethyldithiocarbamate. In *Platinum and Other Metal Complexes in Cancer Chemotherapy*; Nicolini, M., Ed.; Martinus Nijhoff Publishing: Boston, MA, 1988; pp 216–227.
 (20) Faraglia, G.; Fregona, D.; Sitran, S.; Giovagnini, L.; Marzano, C.; Baccichetti, F.; Casellato, U.; Graziani, R. *J. Inorg. Biochem.* **2001**, *83*, 31–40.
 (21) Marzano, C.; Fregona, D.; Baccichetti, F.; Trevisan, A.; Giovagnini, L.; Bordin, F. *Chem.-Biol. Interact.* **2002**, *140*, 215–229.
 (22) Marzano, C.; Trevisan, A.; Giovagnini, L.; Fregona, D. *Toxicol. In Vitro* **2002**, *16*, 413–419.

potassium tetrachloro- and tetrabromoaurate(III) (Alfa Aesar) were used as received. Anhydrous methanol (used for reactions in the drybox) was obtained by drying with CaSO_4 and subsequent fractional distillation. All other reagents and solvents were of high purity and were used as purchased without any further purification.

Synthesis of [(DMDT)AuX₂] (X = Cl, Br). A solution of DMDT sodium salt (1.3 mmol) in water (3 mL) was dropwise added under continuous stirring to an aqueous solution (2 mL) of KAuX_4 (X = Cl, Br; 1.3 mmol), yielding a yellow (X = Cl)/reddish-brown (X = Br) precipitate that was filtered out, washed with water, and, finally, dried in a desiccator with P_4O_{10} , the final yield being 73–80%.

Dichloro(*N,N*-dimethyldithiocarbamato- $\kappa\text{S},\kappa\text{S}'$)gold(III). Anal. Calcd for $\text{C}_3\text{H}_6\text{AuCl}_2\text{NS}_2$ ($M_r = 388.09$ g mol⁻¹): C, 9.29; H, 1.56; N, 3.61; S, 16.53; Cl, 18.27. Found: C, 9.32; H, 1.51; N, 3.54; S, 16.48; Cl, 18.19. The complex is soluble in DMSO, DMF, and nitromethane and slightly soluble in acetonitrile. Mp = 254.8 °C (dec). Λ_M (CH_3NO_2) = 8.91 Ω^{-1} cm² mol⁻¹. FT-IR (KBr, $\tilde{\nu}_{\text{max}}$, cm⁻¹): $\nu(\text{N-CSS}) = 1576$; $\nu_{\text{as}}(\text{SCS}) = 1049$, 551; $\nu_{\text{as}}(\text{SAuS}) = 409$, 382; $\nu_{\text{as}}(\text{ClAuCl}) = 355$, 342. ¹H NMR (400 MHz, DMSO-*d*₆; δ , ppm): 3.37 (6H, s, CH₃N). ¹³C NMR (400 MHz, DMSO-*d*₆; δ , ppm): 40.3 (CH₃N); 193.9 (CSS).

Dibromo(*N,N*-dimethyldithiocarbamato- $\kappa\text{S},\kappa\text{S}'$)gold(III). Anal. Calcd for $\text{C}_3\text{H}_6\text{AuBr}_2\text{NS}_2$ ($M_r = 476.99$ g mol⁻¹): C, 7.55; H, 1.27; N, 2.94; S, 13.45; Br, 33.50. Found: C, 7.65; H, 1.31; N, 2.83; S, 13.62; Br, 33.39. The complex is soluble in DMSO, DMF, and nitromethane and slightly soluble in acetonitrile. Mp = 263.8 °C (dec). Λ_M (CH_3NO_2) = 8.50 Ω^{-1} cm² mol⁻¹. FT-IR (KBr, $\tilde{\nu}_{\text{max}}$, cm⁻¹): $\nu(\text{N-CSS}) = 1577$; $\nu_{\text{as}}(\text{SCS}) = 1048$, 549; $\nu_{\text{as}}(\text{SAuS}) = 404$, 380; $\nu_{\text{as}}(\text{BrAuBr}) = 253$, 227. ¹H NMR (400 MHz, DMSO-*d*₆; δ , ppm): 3.37 (6H, s, CH₃N). ¹³C NMR (400 MHz, DMSO-*d*₆; δ , ppm): 40.5 (CH₃N); 194.1 (CSS).

Synthesis of the DMDTM Ligand. The DMDTM ligand was prepared according to a modified literature method.²³ DMDT sodium salt (28.7 mmol) was dissolved in an ethanol/water (3/2 v/v) mixture (5 mL) under continuous stirring at 80 °C. After complete dissolution, the solution was slowly cooled to room temperature and dropwise treated with CH_3I (28.7 mmol). After 1 h of stirring, the solution was treated with water to incipient precipitation yielding, after 1 night at 4 °C, a white solid that was filtered off and washed with water. A further fraction of white solid was also obtained by treating the mother solution with water and leaving it at 4 °C for other 24 h. The two obtained fractions were then recrystallized from ethanol/water and dried in a desiccator with P_4O_{10} , the final yield being 85%.

***N,N*-Dimethyldithiocarbamic Acid Methyl Ester.** Anal. Calcd for $\text{C}_4\text{H}_9\text{NS}_2$ ($M_r = 135.25$ g mol⁻¹): C, 35.52; H, 6.71; N, 10.36; S, 47.42. Found: C, 35.30; H, 6.63; N, 10.21; S, 47.60. The compound is soluble in methanol, ethanol, chloroform, dichloromethane, acetone, DMSO, pentane, benzene, diethyl ether, acetonitrile, DMF, and nitromethane. Mp = 44.8–45.1 °C. Λ_M (CH_3NO_2) = 2.03 Ω^{-1} cm² mol⁻¹. FT-IR (KBr, $\tilde{\nu}_{\text{max}}$, cm⁻¹): $\nu(\text{N-CSS}) = 1508$; $\nu_{\text{as}}(\text{S=C-S}) = 998$, 961; $\nu(\text{C-S(CH}_3)) = 445$. ¹H NMR (400 MHz, CDCl_3 ; δ , ppm): 2.63 (3H, s, CH₃S); 3.37 (3H, s, CH₃N); 3.55 (3H, s, CH₃N). ¹³C NMR (400 MHz, CDCl_3 ; δ , ppm): 20.4 (CH₃S); 41.3 (CH₃N); 45.3 (CH₃N); 198.4 (CSS).

Synthesis of [(DMDTM)AuX₂] (X = Cl, Br). In a typical preparation, a solution of DMDTM (0.71 mmol) in anhydrous methanol (2 mL) was dropwise added, in a drybox with continuous stirring at room temperature, to a solution of KAuX_4 (X = Cl, Br;

0.71 mmol) in anhydrous methanol (2 mL). The solution was then cooled at 0 °C, and after a few minutes, the product began to separate as reddish-brown needles. After 1 h of stirring, the precipitated substance was filtered off, washed with cool water, and dried in vacuo with P_4O_{10} to obtain a reddish-brown powder, the final yield being 65–68%.

Trichloro(*S*-methyl-*N,N*-dimethyldithiocarbamato-*S'*)gold(III). Anal. Calcd for $\text{C}_4\text{H}_9\text{AuCl}_3\text{NS}_2$ ($M_r = 438.58$ g mol⁻¹): C, 10.95; H, 2.07; N, 3.19; S, 14.62; Cl, 24.25. Found: C, 10.78; H, 2.00; N, 3.08; S, 14.37; Cl, 24.14. The complex is soluble in chloroform, dichloromethane, acetone, DMSO, benzene, acetonitrile, DMF, and nitromethane. Mp = 89.1 °C (dec). Λ_M (CH_3NO_2) = 9.92 Ω^{-1} cm² mol⁻¹. FT-IR (KBr, $\tilde{\nu}_{\text{max}}$, cm⁻¹): $\nu(\text{N-CSS}) = 1548$; $\nu_{\text{as}}(\text{S=C-S}) = 1053$, 985; $\nu(\text{C-S(CH}_3)) = 433$; $\nu(\text{Au-S(=C)}) = 317$; $\nu_{\text{as}}(\text{AuCl}_3) = 356$, 337. ¹H NMR (400 MHz, CDCl_3 ; δ , ppm): 2.99 (3H, s, CH₃S); 3.78 (3H, s, CH₃N); 3.95 (3H, s, CH₃N). ¹³C NMR (400 MHz, CDCl_3 ; δ , ppm): 22.2 (CH₃S); 46.1 (CH₃N); 50.1 (CH₃N); 194.1 (CSS).

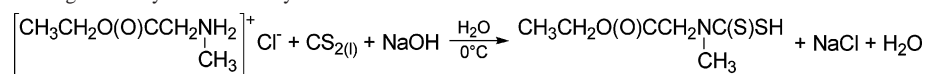
Tribromo(*S*-methyl-*N,N*-dimethyldithiocarbamato-*S'*)gold(III). Anal. Calcd for $\text{C}_4\text{H}_9\text{AuBr}_3\text{NS}_2$ ($M_r = 571.93$ g mol⁻¹): C, 8.40; H, 1.59; N, 2.45; S, 11.21; Br, 42.91. Found: C, 8.39; H, 1.38; N, 2.51; S, 11.34; Br, 43.08. The complex is soluble in chloroform, dichloromethane, acetone, DMSO, benzene, acetonitrile, DMF, and nitromethane. Mp = 108.2 °C (dec). Λ_M (CH_3NO_2) = 7.67 Ω^{-1} cm² mol⁻¹. FT-IR (KBr, $\tilde{\nu}_{\text{max}}$, cm⁻¹): $\nu(\text{N-CSS}) = 1548$; $\nu_{\text{as}}(\text{S=C-S}) = 1049$, 980; $\nu(\text{C-S(CH}_3)) = 432$; $\nu(\text{Au-S(=C)}) = 301$; $\nu_{\text{as}}(\text{AuBr}_3) = 252$, 225. ¹H NMR (400 MHz, CDCl_3 ; δ , ppm): 2.95 (3H, s, CH₃S); 3.65 (3H, s, CH₃N); 3.87 (3H, s, CH₃N). ¹³C NMR (400 MHz, CDCl_3 ; δ , ppm): 22.3 (CH₃S); 45.3 (CH₃N); 50.0 (CH₃N); 194.2 (CSS).

Synthesis of [(DMDTM)AuX] (X = Cl, Br). Gold(I) DMDTM derivatives were prepared with a method similar to that of the corresponding gold(III) derivatives. These complexes were obtained by reaction of KAuX_4 (X = Cl, Br) with DMDTM ligand in 1:2 molar ratio ($\text{KAuX}_4/\text{DMDTM} = 0.79/1.57$ mmol). After 24 h of stirring at 0 °C, the initial reddish-brown precipitate turned to yellow. The compound was then filtered off, washed with cool water, and dried in a desiccator with P_4O_{10} , the final yield being 85–90%. This reaction involving reduction of gold(III) to gold(I) by the dithiocarbamate ester is similar to the reaction occurring between gold(III) halogeno complexes and dialkyl sulfides.¹⁰

Chloro(*S*-methyl-*N,N*-dimethyldithiocarbamato-*S'*)gold(I). Anal. Calcd for $\text{C}_4\text{H}_9\text{AuClNS}_2$ ($M_r = 367.67$ g mol⁻¹): C, 13.07; H, 2.47; N, 3.81; S, 17.44; Cl, 9.64. Found: C, 13.12; H, 2.43; N, 3.79; S, 17.31; Cl, 9.79. The complex is soluble in DMSO, acetonitrile, DMF, and nitromethane and slightly soluble in chloroform. Mp = 152.7 °C (dec). Λ_M (CH_3NO_2) = 6.69 Ω^{-1} cm² mol⁻¹. FT-IR (KBr, $\tilde{\nu}_{\text{max}}$, cm⁻¹): $\nu(\text{N-CSS}) = 1528$; $\nu_{\text{as}}(\text{S=C-S}) = 1059$, 989; $\nu(\text{C-S(CH}_3)) = 442$; $\nu(\text{Au-S(=C)}) = 289$; $\nu(\text{AuCl}) = 316/307$. ¹H NMR (400 MHz, CDCl_3 ; δ , ppm): 2.96 (3H, s, CH₃S); 3.56 (3H, s, CH₃N); 3.91 (3H, s, CH₃N). ¹³C NMR (400 MHz, CDCl_3 ; δ , ppm): 21.4 (CH₃S); 44.6 (CH₃N); 48.2 (CH₃N); 199.1 (CSS).

Bromo(*S*-methyl-*N,N*-dimethyldithiocarbamato-*S'*)gold(I). Anal. Calcd for $\text{C}_4\text{H}_9\text{AuBrNS}_2$ ($M_r = 412.12$ g mol⁻¹): C, 11.66; H, 2.20; N, 3.40; S, 15.56; Br, 19.39. Found: C, 11.61; H, 2.22; N, 3.33; S, 15.40; Br, 19.49. The complex is soluble in DMSO and slightly soluble in chloroform, dichloromethane, and nitromethane. Mp = 152.0 °C (dec). Λ_M (CH_3NO_2) = 9.33 Ω^{-1} cm² mol⁻¹. FT-IR (KBr, $\tilde{\nu}_{\text{max}}$, cm⁻¹): $\nu(\text{N-CSS}) = 1523$; $\nu_{\text{as}}(\text{S=C-S}) = 1051$, 982; $\nu(\text{C-S(CH}_3)) = 443$; $\nu(\text{Au-S(=C)}) = 278$; $\nu(\text{AuBr}) = 240$. ¹H NMR (400 MHz, CDCl_3 ; δ , ppm): 2.82 (3H, s,

(23) Ainley, A. D.; Davis, W. H.; Gudgeon, H.; Harland, J. C.; Shixton, W. A. *J. Chem. Soc.* **1944**, 147–151.

Scheme 1. Reaction Leading to the Synthesis of Ethylsarcosinedithiocarbamic Acid

CH₃S); 3.48 (3H, s, CH₃N); 3.77 (3H, s, CH₃N). ¹³C NMR (400 MHz, CDCl₃; δ, ppm): 21.0 (CH₃S); 43.1 (CH₃N); 47.0 (CH₃N); 198.8 (CSS).

Synthesis of [(ESDT)AuX₂] (X = Cl, Br). A water solution (3 mL) of ethylsarcosinehydrochloride (1.42 mmol) cooled at 0 °C was dropwise treated under continuous stirring with cool CS₂ (1.43 mmol) and an aqueous solution (1 mL) of NaOH (1.42 mmol). After 1 h, the pH value turned from 10 to 6 according to the reaction shown in Scheme 1. The solution thus obtained was slowly added under stirring to an aqueous cool (0 °C) solution (2 mL) of KAuX₄ (X = Cl, Br; 0.70 mmol), leading to the immediate precipitation of a yellow-ochre (X = Cl)/reddish-brown (X = Br) solid that was filtered off, washed with water, and dried in a desiccator with P₄O₁₀, the final yield being 82–85%.

Dichloro[ethyl *N*-(dithiocarboxy-κS,κS′)-*N*-methylglycinato]-gold(III). Anal. Calcd for C₆H₁₀AuCl₂NO₂S₂ (*M_r* = 460.16 g mol⁻¹): C, 15.66; H, 2.19; N, 3.04; S, 13.94; Cl, 15.41. Found: C, 15.77; H, 2.09; N, 2.98; S, 13.81; Cl, 15.33. The complex is soluble in methanol, chloroform, dichloromethane, acetone, DMSO, acetonitrile, DMF, and nitromethane and slightly soluble in ethanol. *M_p* = 176.5–177.5 °C. Λ_{M} (CH₃NO₂) = 4.56 Ω⁻¹ cm² mol⁻¹. FT-IR (KBr, $\tilde{\nu}_{\text{max}}$, cm⁻¹): ν(N–CSS) = 1570; ν(C=O) = 1736; ν(C–OEt) = 1218; ν_{a,s}(SCS) = 1001, 578; ν_{a,s}(SAuS) = 403, 387; ν_{a,s}(ClAuCl) = 359, 341. ¹H NMR (400 MHz, acetone-*d*₆; δ, ppm): 1.28 (3H, t, CH₃); 3.57/3.61 (3H, s, CH₃N); 4.27 (2H, q, CH₂O); 4.80/4.81 (2H, s, CH₂N). ¹³C NMR (400 MHz, acetone-*d*₆; δ, ppm): 14.3 (CH₃); 39.9/40.5 (CH₃N); 53.8/54.2 (CH₂N); 63.2 (CH₂O); 165.7 (COO); 197.8/201.0 (CSS).

Dibromo[ethyl *N*-(dithiocarboxy-κS,κS′)-*N*-methylglycinato]-gold(III). Anal. Calcd for C₆H₁₀AuBr₂NO₂S₂ (*M_r* = 549.06 g mol⁻¹): C, 13.13; H, 1.84; N, 2.55; S, 11.68; Br, 29.11. Found: C, 13.24; H, 1.79; N, 2.48; S, 11.69; Br, 28.92. The complex is soluble in methanol, chloroform, dichloromethane, acetone, DMSO, acetonitrile, DMF, and nitromethane and slightly soluble in ethanol. *M_p* = 182.5–183.5 °C. Λ_{M} (CH₃NO₂) = 6.10 Ω⁻¹ cm² mol⁻¹. FT-IR (KBr, $\tilde{\nu}_{\text{max}}$, cm⁻¹): ν(N–CSS) = 1560; ν(C=O) = 1739; ν(C–OEt) = 1212; ν_{a,s}(SCS) = 1001, 575; ν_{a,s}(SAuS) = 405, 382; ν_{a,s}(BrAuBr) = 251, 228. ¹H NMR (400 MHz, acetone-*d*₆; δ, ppm): 1.28 (3H, t, CH₃); 3.56/3.61 (3H, s, CH₃N); 4.28 (2H, q, CH₂O); 4.7/4.80 (2H, s, CH₂N). ¹³C NMR (400 MHz, acetone-*d*₆; δ, ppm): 14.3 (CH₃); 39.5/40.5 (CH₃N); 53.5/54.3 (CH₂N); 63.2 (CH₂O); 165.9 (COO); 197.3/200.8 (CSS).

Synthesis of [(ESDT)Au]₂. Reduction of gold(III) to gold(I) was achieved by following two different methods.

Method 1. According to the literature method,^{24–26} the gold(I) intermediate was prepared by starting with KAuX₄ (X = Cl, Br; 1.3 mmol) in aqueous solution (2 mL) cooled at 0 °C and dropwise treating it with a water solution of 0.1 M Na₂SO₃ under vigorous stirring until the solution became colorless (complete reduction).

Method 2. Following a more effective method,²⁷ reduction to gold(I) was achieved by dropwise treating a water solution (3 mL) of KAuX₄ (X = Cl, Br; 0.69 mmol) with an aqueous solution (2

mL) of ethyl 2-hydroxyethyl sulfide (0.15 mL ≅ 1.44 mmol) under vigorous stirring until the solution became colorless.

In both cases, the colorless solution of gold(I) thus obtained was treated at 0 °C under stirring with an aqueous solution of ethylsarcosinedithiocarbamic acid in 1:2 metal-to-ligand molar ratio, as previously described for the gold(III) ESDT derivatives, yielding, after 24 h of stirring, a gray-violet solid that was filtered off, washed with water, and dried in a desiccator with P₄O₁₀ (final yield: 71–78%).

Bis[ethyl *N*-(dithiocarboxy-κS,κS′)-*N*-methylglycinato]digold(I). Anal. Calcd for C₁₂H₂₀Au₂N₂O₄S₄ (*M_r* = 778.50 g mol⁻¹): C, 18.51; H, 2.59; N, 3.60; S, 16.48. Found: C, 18.64; H, 2.42; N, 3.58; S, 16.63. This complex is soluble in DMSO and slightly soluble in nitromethane. *M_p* = 168.7 °C (dec). Λ_{M} (CH₃NO₂) = 2.73 Ω⁻¹ cm² mol⁻¹. FT-IR (KBr, $\tilde{\nu}_{\text{max}}$, cm⁻¹): ν(N–CSS) = 1481; ν(C=O) = 1734; ν(C–OEt) = 1207; ν_{a,s}(SCS) = 1013, 499; ν_{a,s}-(SAuS) = 340, 321. ¹H NMR (400 MHz, DMSO-*d*₆; δ, ppm): 1.22 (6H, t, CH₃); 3.50 (6H, s, CH₃N); 4.18 (4H, q, CH₂O); 4.69 (4H, s, CH₂N). ¹³C NMR (400 MHz, DMSO-*d*₆; δ, ppm): 13.7 (CH₃); 46.6 (CH₃N); 59.5 (CH₂N); 62.7 (CH₂O); 166.3 (COO); 204.4 (CSS).

Instrumentation. Conductivity measurements were carried out with an Amel 134-type conductivity bridge for freshly prepared 10⁻³ M solutions in nitromethane at 25.0 ± 0.1 °C.

FT-IR spectra were recorded in Nujol between two polyethylene tablets on a Nicolet Vacuum Far FT-IR 20F spectrophotometer for the range 600–50 cm⁻¹ and in solid KBr on a Nicolet FT-IR 55XC spectrophotometer for the range 4000–400 cm⁻¹.

Mono- and bidimensional NMR spectra were recorded in the appropriate deuterated solvent on a Bruker Avance DRX400 spectrophotometer equipped with a Silicon Graphics O2 workstation operating in Fourier transform, using tetramethylsilane (TMS) as internal standard.

Elemental analyses were performed with a Perkin-Elmer 2400 CHN microanalyzer; S, Cl, and Br were determined by the Schöniger method.

Electronic spectra were recorded in the range 190–900 nm with a Perkin-Elmer Lambda 15 double beam spectrophotometer, using fresh (2–5) × 10⁻⁵ M solutions of the samples in the appropriate solvent.

Thermogravimetric (TG) and differential scanning calorimetry (DSC) curves were recorded with a TA Instruments thermobalance equipped with a DSC 2929 calorimeter; the measurements were carried out in the range 25–1400 °C in alumina crucibles under air (flux rate: 30 cm³ min⁻¹) and at a heating rate of 10 °C min⁻¹, using alumina as reference.

All electrochemical experiments were performed in anhydrous deoxygenated acetonitrile solutions with 0.2 M tetraethylammonium perchlorate (TEAP) as supporting electrolyte at 25.0 ± 0.1 °C, using a conventional three-electrode liquid-jacket cell; the complexes concentration was 1–3 mM. Cyclic voltammetry (CV) measurements were carried out with an Amel 551 potentiostat modulated by an Amel 566 function generator. The recording device was an Amel 863X-Y model recorder. The working electrode was a planar gold microelectrode freshly coated with mercury (ca. 0.4 mm²) surrounded by a platinum spiral counter electrode. Controlled electrolyses were carried out with an Amel 552 potentiostat linked to an Amel 731 digital integrator. The working electrode was a

(24) Åkerström, S. *Ark. Kemi* **1959**, *14*, 387–401.

(25) Dobrowolski, J.; Bodowski, Z.; Kwiatkowska, I. *Rocz. Chem.* **1976**, *50*, 53–59.

(26) Blaauw, H. J.; Nivard, R. J.; van der Kerk, G. J. M. *J. Organomet. Chem.* **1964**, *2*, 235–244.

(27) Bishop, P.; Marsh, P.; Brisdon, A. K.; Brisdon, B. J.; Mahon, M. F. *J. Chem. Soc., Dalton Trans.* **1998**, 675–682.

mercury pool (ca. 12 cm²), and the counter electrode was external, the connection being made through an appropriate salt bridge. In both cases, a saturated calomel electrode (SCE) in acetonitrile, separated from the test solution by a 0.2 M TEAP solution in acetonitrile sandwiched between two fritted disks, was used as the reference electrode. Potentials were recorded and given vs SCE but were standardized against the ferrocenium/ferrocene redox couple, to define a uniform value of +0.400 V vs SCE as the ferrocene potential.

Cell Lines and Culture Conditions. Human squamous cervical adenocarcinoma HeLa cells (kindly provided by Prof. F. Majone, Department of Biology, University of Padua, Padua, Italy) and human colon adenocarcinoma LoVo cells (American Type Culture Collection, ATCC) were grown in Hams-F12 medium (Euroclone). Human leukemic promyelocytes HL60 cells, human Burkitt's lymphoma Daudi cells, human malignant melanoma MeWo cells (ATCC), human ovarian carcinoma cisplatin-sensitive 2008 and cisplatin-resistant C13* cells (kindly provided by Prof. G. Marverti, Department of Biomedical Sciences, University of Modena, Modena, Italy), and human squamous cervix carcinoma cisplatin-sensitive A431 and cisplatin-resistant A431-R cells (kindly provided by Prof. F. Zunino, National Cancer Institute, Milan, Italy) were grown as a suspension in RPMI-1640 medium (Celbio). Human nonsmall lung adenocarcinoma A549 cells (ATCC) were cultured in D-MEM medium (Euroclone). Human osteosarcoma cisplatin-sensitive U2OS and cisplatin-resistant U2OS-R cells (kindly provided by Prof. F. Zunino) were grown in McCoy's medium (Euroclone). In all cases the growth medium was supplemented with antibiotics penicillin (50 units mL⁻¹) and streptomycin (50 µg mL⁻¹) and 10% complemented fetal calf serum (Euroclone). The growth of all the cell cultures was accomplished in 25 mL Falcon bottles at 37 °C under continuous flux of a 5% carbon dioxide and moisture-enriched atmosphere. Trypsin (0.25%, Boehringer) was routinely used for subculture.

In Vitro Cytotoxicity Studies. The MTT (tetrazolium salt reduction) test was undertaken according to the method described by Abbey et al.²⁸ The cells (3 × 10³ cells mL⁻¹ for 2008 and C13* cells; 5 × 10³ cells mL⁻¹ for HeLa, A431, A431-R, U2OS, and U2OS-R cells; 8 × 10³ cells mL⁻¹ for HL60, LoVo, MeWo, and Daudi cells) were seeded in 96-well microplates in the appropriate growth medium (100 µL) and then incubated at 37 °C in a 10% carbon dioxide controlled atmosphere. After 24 h, the medium was removed and replaced with a fresh medium containing the compounds to be studied, previously dissolved in DMSO, at increasing concentrations (6.25/12.5/25/50/100 µM); for comparison purpose, cisplatin (Sigma Chemical Co.) was also tested under the same experimental conditions. Quadruplicate cultures were established for each treatment. After other 24 h, each well was treated with 10 µL of a 5 mg mL⁻¹ MTT (3-(4,5-dimethylthiazole-2-yl)-2,5-diphenyltetrazolium bromide, Sigma Chemical Co.) saline solution, and after 5 h of incubation, 100 µL of a sodium dodecyl sulfate (SDS) in 0.1 M HCl solution was added. After an overnight incubation, the inhibition of cell growth by the various complexes was detected by measuring the absorbance of each well at 570 nm using a Camberra-Packard microplate reader. The cytotoxic effect of each tested compound was evaluated by the percentage of living cells present in the sample in relation to the cells treated with the solvent only. Dose-response curves were then calculated for the chemicals over a range of concentrations, enabling IC₅₀ (concentra-

tion of chemical resulting in 50% inhibition of cell growth) values to be obtained.

Clonal Growth Test. The (1–2.5) × 10⁵ cells mL⁻¹ (HeLa, 2008/C13*, A431/A431-R) were seeded in 60-mm Petri dishes in 10 mL of the appropriate growth medium (Hams-F12 for HeLa cells and RPMI-1640 for the remaining cell lines). After 24 h, the medium was removed and replaced with a fresh one containing the compounds to be studied, previously dissolved in DMSO, at the appropriate concentration (1.5/3.125/6.25/12.5 µM); cells were then incubated for 3 h at 37 °C in the dark under controlled atmosphere. Triplicate cultures were established for each treatment; for comparison purpose, cisplatin was also tested under the same experimental conditions. The dishes were then washed with PBS solution, and aliquots of 100 cells from each treated and untreated culture were seeded in complete growth medium and incubated for 10 days at 37 °C in a 5% carbon dioxide atmosphere. The colonies were then stained and counted, discarding colonies with less than 50 cells. The efficiency of clonal growth (that is, the ratio between the number of colonies formed and the number of cells seeded) was then calculated.

Results and Discussion

Synthesis of the Complexes. The gold(III) DMDT derivatives have been obtained by direct reaction in water between KAUX₄ and DMDT sodium salt in 1:1 molar ratio to give the corresponding stoichiometric adducts [(DMDT)-AuX₂] (X = Cl, Br).

By reaction of the DMDTM ligand with KAUX₄ species in 1:1 and 2:1 molar ratio, we have obtained the S-methylated complexes of the type [(MSDTM)AuX₃] and [(MSDTM)-AuX] (X = Cl, Br), respectively, in which the dithiocarbamate ligand coordinates the metal center through the thiocarbonyl sulfur-donating atom.

Gold(III) ESDT derivatives have been prepared by a template reaction between KAUX₄, ESHCl (ethylsarcosine-hydrochloride), CS₂, and NaOH in 1:2:2:2 molar ratio, leading to pure 1:1 metal-to-ligand species of the type [(ESDT)AuX₂] (X = Cl, Br). The gold(I) analogue [(ESDT)-Au]₂ has been synthesized by the same template reaction, following the complete reduction of KAUX₄ to the corresponding gold(I) precursor KAUX₂. In Chart 2 the chemical drawings of all the complexes reported in this work are shown.

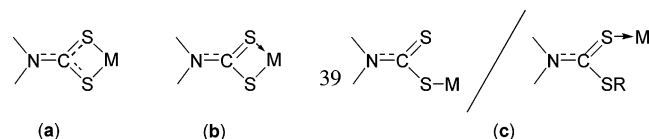
As concerns the template synthesis of ESDT derivatives, a separate discussion is required. The main synthetic route to dithiocarbamates is based on the interaction between the corresponding amine and carbon disulfide in the presence of a strong base.²⁹ This process can even take place in the absence of a strong base, but in this case, the yield of dithiocarbamate corresponds to about half the amount of consumed amine in the presence of a strong base; indeed, the base-catalyzed reaction makes an essential contribution to the dithiocarbamate formation rate.³⁰ In our studies, this reaction involves the base-catalyzed nucleophilic addition of the amino moiety of the investigated α-amino acid (ethylsarcosine) to carbon disulfide in aqueous medium. As

(28) Alley, M. C.; Scudiero, D. A.; Monks, A.; Hursey, M. L.; Czerwinski, M. J.; Fine, D. L.; Abbott, B. J.; Mayo, J. G.; Shoemaker, R. H.; Boyd, M. R. *Cancer Res.* **1988**, *48*, 589–601.

(29) Shkaraputa, L. N.; Kononov, A. V.; Polyakov, A. D. *Ukr. Chem. J.* **1991**, *9*, 979–989.

(30) Vasiliev, A. N.; Polackov, A. D. *Molecules* **2000**, *5*, 1011–1013.

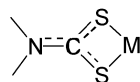
Chart 3. Different Ways of Metal–Sulfur Binding in Dithiocarbamate Complexes: Symmetrical Bidentate (a); Asymmetrical Bidentate (b); Monodentate (c)



into account inductive and hyperconjugation effects of the various alkyl groups, together with their different steric hindrance and spatial rearrangement.⁴⁹

To discern the bonding type of the dithiocarbamate ligands in their complexes, the Bonati–Ugo method⁵⁰ is, by far, the most popular one. It consists of tracing the 940–1060 cm^{-1} spectral region, where the $\nu(\text{C}-\text{S})$ modes are thought to appear. In fact, the bands due to the $-\text{CSS}$ moiety are usually coupled to other vibrations and are very sensitive to the environment around this group, but they are also useful to distinguish between monodentate and bidentate coordination.⁵¹ The presence of only one band in the investigated region, commonly attributed to a $\nu_a(\text{SCS})$ mode, is assumed to indicate a completely symmetrically bonding of the dithiocarbamate ligand, acting in a bidentate mode (Chart 3a), and this is the case of all the gold(III) DMDT and ESDT derivatives. Conversely, a split band indicates an asymmetrically bonded bidentate ligand ($\Delta\tilde{\nu} < 20 \text{ cm}^{-1}$, Chart 3b) or a monodentate bound ligand ($\Delta\tilde{\nu} > 20 \text{ cm}^{-1}$, Chart 3c). In all the DMDTM gold(III)/gold(I) complexes, the presence of two bands split of 33–42 cm^{-1} in the above-discussed range supports the idea of a monodentate behavior of the dithiocarbamate moiety, metal coordination occurring through the thiocarbonyl sulfur atom.⁴⁴

The band recorded for both the complexes and the free dithiocarbamate precursors in the 420–630 cm^{-1} range can be ascribed to the contribution of $\nu(\text{C}-\text{S}) + \delta(\text{SCS})$ vibrational modes, and the frequencies here reported are in large agreement with literature data.^{27,42–44,52} It is interesting to point out that the bands in this range involve some ring



deformations, as demonstrated by detailed FT-IR isotopic studies on dithiocarbamate complexes of $^{58}\text{Ni}(\text{II})$, $^{62}\text{Ni}(\text{II})$, $^{63}\text{Cu}(\text{II})$, and $^{65}\text{Cu}(\text{II})$.⁵³

New bands, absent in the spectra of the starting materials, are observed in the 250–420 cm^{-1} range, and they can be assigned to the metal–sulfur stretching modes according to the normal coordinate analysis of the dithiocarbamate

complexes and previous works on gold derivatives.^{42,43} It is worth noting that $\nu(\text{Au}-\text{S})$ increases in frequency as the oxidation number of the gold ion increases.^{34,42,43,54} In the same range, other informative bands are detected, attributed to the $\nu(\text{Au}-\text{X})$ ($\text{X} = \text{Cl}, \text{Br}$) modes. These bands are ascribed to the $\text{Au}-\text{X}$ stretching frequencies for terminal halides.^{43,54,55} It is worth observing that in the far FT-IR spectra of all the chloro derivatives, the bands assignable to the $\nu(\text{Au}-\text{Cl})$ vibrations are broad or even doubled because of the isotopic splitting $\nu(\text{Au}-^{35/37}\text{Cl})$. Isotopic splitting is clearer for compounds containing one $\text{Au}-\text{Cl}$ bond than for those containing more than one chlorine atom bound to the same gold center; the fact that there is only one stable isotope of gold (^{197}Au) helps to make $\text{Au}-\text{Cl}$ isotopic splitting more easily observable than in the case of chlorides of elements consisting of a mixture of stable isotopes.⁵⁵

^1H and ^{13}C NMR Spectroscopy. As regards the alkyl groups bound to the dithiocarbamate moiety, ^1H signals are very close for the free precursors (DMDTNa, DMDTM, and ESHCl) and the corresponding complexes. A general shift toward larger δ values is observed from the free DMDTNa and DMDTM to the corresponding gold complexes, probably due to the greater electron density existing on these protons in the former case.⁴¹ In particular, for DMDT derivatives this downfield shift is caused by the lower electron density in the complexes, in which the $-\text{NCSS}$ moiety is neutral, than in the free ligands, in which such a dithiocarbamic group is anionic. Conversely, for carbon atoms a significant shielding of the ^{13}C signals is recorded, in comparison with the free dithiocarbamate ligands, in agreement with data reported in the literature for similar compounds.^{40,41,56}

The main differences are observable for the ^{13}C signals of the dithiocarbamic carbon atoms. The $\delta(\text{N}^{13}\text{CSS})$ values are found in the range 190–215 ppm, and it is generally assumed that they are strongly dependent on both the type of dithiocarbamate–metal bonding and the oxidation state of the metal center.⁵⁷ For high oxidation state transition metal dithiocarbamate derivatives, such as gold(III) ones, the $\delta(\text{N}^{13}\text{CSS})$ values are usually found in the range 193–201 ppm.⁵⁸ On the other hand, for dithiocarbamate complexes of transition metals owing a d^{10} electronic configuration, such as oligomeric complexes of gold(I), the $\delta(\text{N}^{13}\text{CSS})$ values are shifted to lower fields in the range 202–206 ppm.⁵⁹ There is a strong empirical correlation between $\delta(\text{N}^{13}\text{CSS})$ values and the carbon–nitrogen stretching vibrations in the infrared spectra: higher $\nu(\text{N}-\text{CSS})$ values indicate an increased carbon–nitrogen double bond character, which well correlates with lower $\delta(\text{N}^{13}\text{CSS})$ values because of a greater electron density on the $-\text{NCSS}$ moiety. In a semiempirical

(48) Bellamy, L. J. *The Infrared Spectra of Complex Molecules*; Chapman & Hall: London, 1975.
 (49) Brounholtz, J. T.; Ebsworth, E. A. V.; Momm, F. G.; Sheppard, N. J. *Chem. Soc.* **1958**, 2780–2785.
 (50) Bonati, F.; Ugo, R. J. *Organomet. Chem.* **1967**, *10*, 257–268.
 (51) Kellner, R.; Nikolov, G. S.; Trendafilova, N. *Inorg. Chim. Acta* **1984**, *84*, 233–239.
 (52) Radanovic, D. J.; Matovic, Z. D.; Miletic, V. D.; Battaglia, L. P.; Ianelli, S.; Efimenko, I. A.; Ponticelli, G. *Transition Met. Chem.* **1996**, *21*, 169–175.
 (53) Desseyn, H. O.; Fabretti, A. C.; Forghieri, F.; Preti, C. *Spectrochim. Acta* **1985**, *41A*, 1105–1108.

(54) Beurskens, P. T.; Blaauw, H. J. A.; Cras, J. A.; Steggerda, J. J. *Inorg. Chem.* **1968**, *7*, 805–810.
 (55) Coates, G. E.; Parkin, C. J. *Chem. Soc.* **1963**, 421–429.
 (56) Criado, J. J.; Carrasco, A.; Macias, B.; Salas, J. M.; Medarde, M.; Castillo, M. *Inorg. Chim. Acta* **1989**, *160*, 37–42.
 (57) van Gaal, H. L. M.; Diesveld, J. W.; Pijpers, F. W.; van der Linden, J. G. M. *Inorg. Chem.* **1979**, *18*, 3251–3260.
 (58) Willemsse, J.; Cras, J. A.; Steggerda, J. J.; Keyzers, C. P. *Struct. Bonding (Berlin)* **1976**, *28*, 83–88.
 (59) Pijpers, F. W.; Dix, A. H.; van der Linden, J. G. M. *Inorg. Chim. Acta* **1974**, *11*, 41–45.

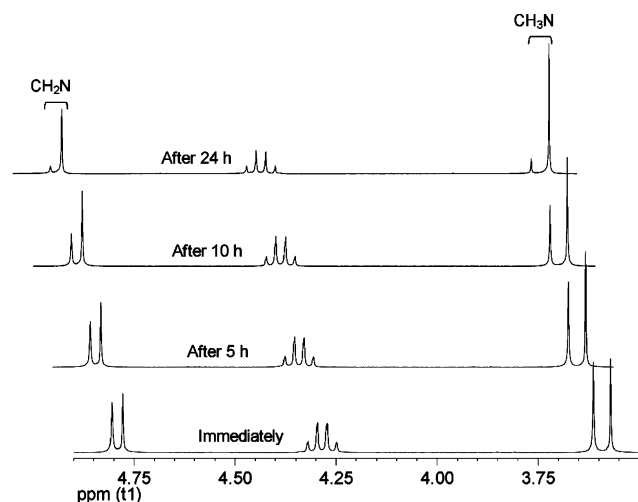


Figure 2. ^1H NMR spectra of $[(\text{ESDT})\text{AuBr}_2]$ in $(\text{CD}_3)_2\text{CO}$ performed at different times.

way, $\delta(\text{N}^{13}\text{CSS})$ could be expressed as a linear function of the sum of CN, CS1, and CS2 π -bond orders, and $\nu(\text{N}-\text{CSS})$ as a linear function of the CN π -bond order.⁵⁷ The sum of the π -bond order is derived to be maximal for equal π bonds and to decrease with increasing inequality of the three π bonds. Therefore, the compounds with high $\nu(\text{N}-\text{CSS})$ values have low CS and low total π -bond orders, thus leading to low $\delta(\text{N}^{13}\text{CSS})$ values, and vice versa. For the free dithiocarbamate ligands, there is no charge compensation on sulfur by coordinated atoms, leading to nearly equal π bonds; this results in extremely low $\nu(\text{N}-\text{CSS})$ values, correlated with $-\text{N}^{13}\text{CSS}$ signals located in the upper limit of δ values. All these considerations are fully consistent with experimental $-\text{N}^{13}\text{CSS}$ carbon signals recorded for the here investigated dithiocarbamate complexes. Moreover, on passage from gold(III) to gold(I) derivatives of the same dithiocarbamate ligand, $\nu(\text{N}-\text{CSS})$ values decrease whereas $\delta(\text{N}^{13}\text{CSS})$ ones increase.

For ESDT derivatives, the NMR signals attributed to the ester moieties are very similar to those of the free ethylsarcosine hydrochloride as the insertion of a dithiocarbamic group does not affect their magnetic environment at all.⁵⁶ On the contrary, it is worth observing that these complexes give rise to isomerization in solution, in particular as concerns the $-\text{CH}_2\text{N}(\text{CH}_3)\text{CSS}$ group. For example, in Figure 2 the ^1H NMR spectra of $[(\text{ESDT})\text{AuBr}_2]$ performed in $(\text{CD}_3)_2\text{CO}$ at different times are reported. At the beginning, two signals are recorded for both *N*-methyl and *N*-methylene protons at 3.56/3.61 and 4.77/4.86 ppm, respectively in 1:1 ratio; in time, the lower field peaks, referred to one of the two isomers, progressively decrease in intensity until their almost complete disappearance within 24 h. The existence of two isomers in solution is also confirmed by both the presence of two signals for $-\text{CSS}$ carbon atom in the $^1\text{H}^{13}\text{C}$ -HMBC spectrum, in which each dithiocarbamic carbon gives rise to a long-range coupling with one of the CH_2N and CH_3N proton signals (Figure 3), and the occurrence of two different dipolar correlations between 3.35 and 4.77 and 3.61–4.80 (CH_3N and CH_2N) ppm chemical shifts in the $^1\text{H}^1\text{H}$ -NOESY spectrum (Figure 4).

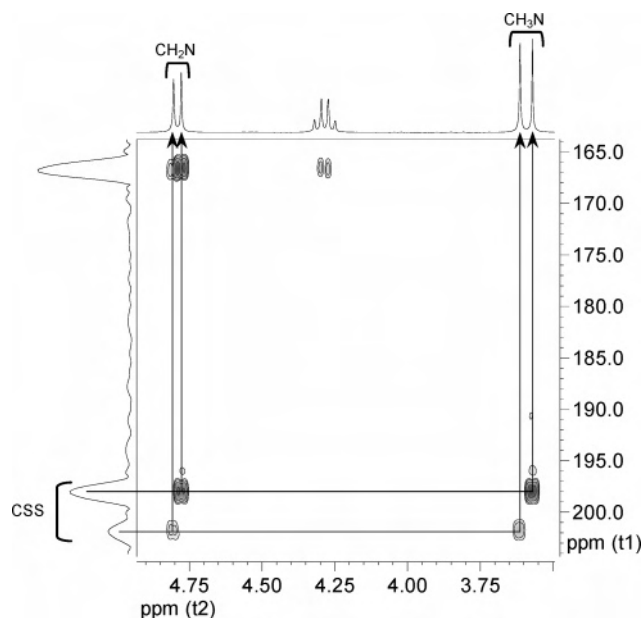


Figure 3. $^1\text{H}^{13}\text{C}$ -HMBC spectrum of $[(\text{ESDT})\text{AuBr}_2]$ in $(\text{CD}_3)_2\text{CO}$ (detailed).

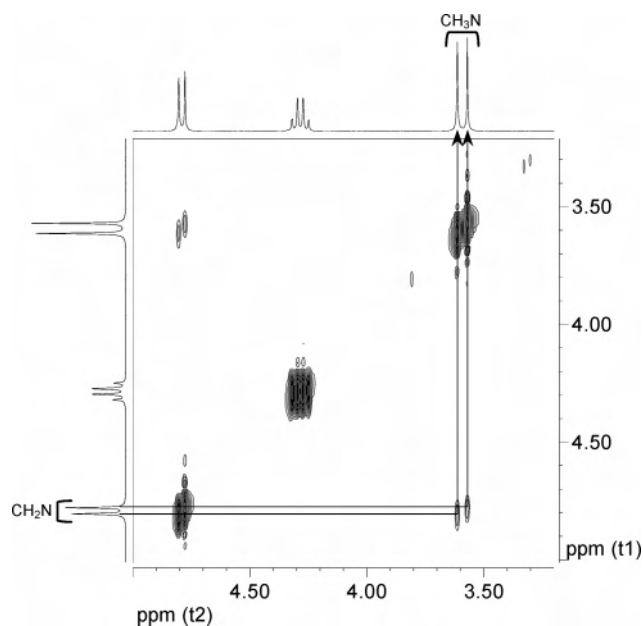
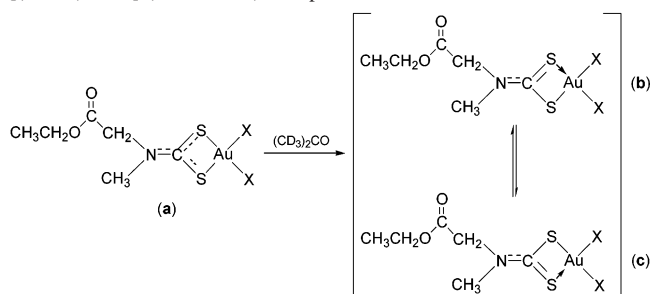


Figure 4. $^1\text{H}^1\text{H}$ -NOESY spectrum of $[(\text{ESDT})\text{AuBr}_2]$ in $(\text{CD}_3)_2\text{CO}$ (detailed).

Remarkably, $[(\text{ESDT})\text{AuX}_2]$ ($\text{X} = \text{Cl}, \text{Br}$) complexes do not own evident stereocenters able to give rise to two different isomers. Anyway, a possible explanation of such an apparently unaccountable behavior may be that these gold(III) dithiocarbamate derivatives have symmetrical dithiocarbamic fragments in the solid state (Scheme 5a), whereas in solution dithiocarbamic sulfur atoms–metal bonding becomes asymmetric (Scheme 5b,c) and this occurrence would be promoted by the solvent. A similar behavior has been already reported in the literature for some gold dithiocarbamate derivatives which have asymmetrical bonded dithiocarbamate fragments in the solid state, whereas ^1H NMR results indicate symmetric bonding in solution.^{57,59} If this change happened in solution, we should be able to discern different NMR signals for each isomer, as we indeed

Scheme 5. Hypothesized Isomerization Reaction in Solution of [(ESDT)AuX₂] (X = Cl, Br) Complexes



do; it must be also reminded that the partial double-bond character of the nitrogen–carbon bond does not allow free rotation around the N–CSS bond, thus leading to slow interconversion between the two hypothesized isomeric forms and to the simultaneous presence of the two species in solution. Remarkably, this behavior has been also observed in DMSO-*d*₆ solutions, but in this case, the initial relative abundance of the two isomeric species (1:1) did not change in time, confirming the crucial role of the solvent in these isomerization reactions.

Conversely, no isomers are present for gold(I) ESDT derivative [(ESDT)Au]₂, whose ¹H/¹³C NMR signal values are similar to those of the gold(III) analogues. The main differences regards the peaks assignable to –CSS carbon atom at 204 ppm, which is slightly deshielded, compared to the same signal of the gold(III) ESDT analogues, and whose value is in good agreement with data reported in the literature for similar binuclear gold(I) dithiocarbamate derivatives.^{27,46,60}

A separate discussion is required for DMDTM derivatives. The ¹H/¹³C NMR spectra of all the DMDTM derivatives display, compared to free DMDTM ligand, downfield shifts of the methyl resonances; these data observed upon complexation are similar to those found for platinum(II) DMDTM complexes,⁶¹ whose crystal structure was determined, and indicate metal coordination through the thiocarbonyl sulfur atom. In both the free DMDTM ligand and its gold(I)/gold(III) derivatives, two different ¹H/¹³C signals are recorded for the two *N*-methyl groups, due to their different chemical environment; the signals at higher fields are attributed to the *N*-methyl group closer to the *S*-methyl atom, whose electronic cloud slightly shield these CH₃N protons.⁶² In Figure 5, the ¹H-¹H-NOESY spectrum of [(DMDTM)AuCl₃] is reported as an example; it is interesting to observe that in both [(DMDTM)AuX₃] and [(DMDTM)AuX] (X = Cl, Br) no dipolar correlation exists between one of the CH₃N group and the CH₃S protons, meaning that they are not in a close spatial relationship. This evidence confirms the hypothesis exposed in previous studies that the conformation with CH₃S in a *cis* position to the C=S group is the only one accessible.^{44,63,64}

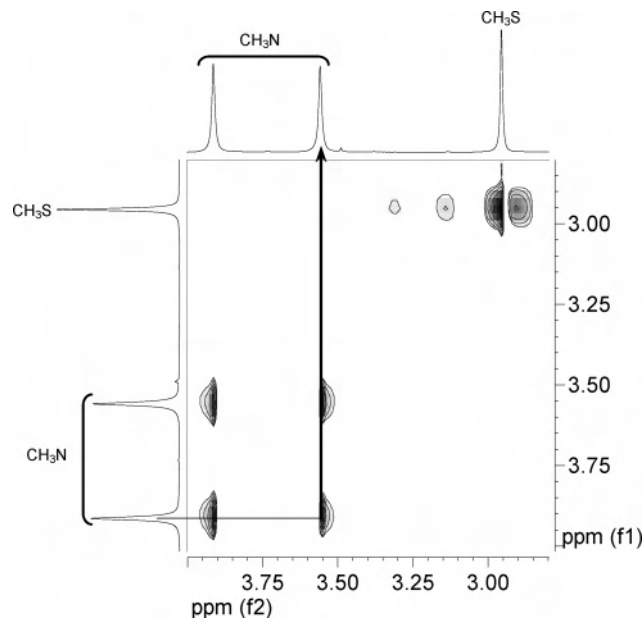


Figure 5. ¹H-¹H-NOESY spectrum of [(DMDTM)AuCl₃] in CDCl₃.

The chloroform solutions of [(DMDTM)AuX] (X = Cl, Br) complexes are not stable at all. Formation of metallic gold and darkening of the solutions upon standing indicate that disproportion of gold(I) takes place, according to the reaction



This is apparent, for example, in the ¹H NMR spectrum of [(DMDTM)AuBr] in which, after 12 h, signals at $\delta = 2.95$, 3.65, and 3.87 ppm and $\delta = 2.63$, 3.37, and 3.55 ppm appear, identical with those displayed by fresh chloroform solutions of [(DMDTM)AuBr₃] and free DMDTM ligand, respectively. The same behavior has been observed for the corresponding chloro-analogue [(DMDTM)AuCl].

UV–Vis Spectroscopy. Optical electronic absorption spectra in solution generally show a similar pattern for all the complexes, and the main features have been collected in Table 1. Spectra of [(DMDT)AuCl₂], [(DMDT)AuBr₂], and [(ESDT)Au]₂ have not been recorded because of their poor solubility in proper solvents for this characterization technique.

Band I has not been undoubtedly ascribed in the literature to a particular electronic transition, and it is still the subject of debate: sometimes it has been assigned either to an intraligand $\pi^* \leftarrow \pi$ transition located in the –NCSS moiety⁶⁵ or to intraligand $p \leftarrow d$ transitions between levels originated by sulfur atoms,^{39,66} and it has even been unassigned in most cases.⁶⁷

(60) Fernandez, E. J.; Lopez de Luzuriaga, J. M.; Monge, M.; Olmos, E.; Gimeno, M. C.; Laguna, A.; Jones, P. G. *Inorg. Chem.* **1998**, *37*, 5532–5536.

(61) Clemente, D. A.; Faraglia, G.; Sindellari, L.; Trincia, L. *J. Chem. Soc., Dalton Trans.* **1987**, 1823–1826.

(62) Gayathry Devi, K. R.; Sathyanarayana, D. N. *Indian J. Chem.* **1980**, *19A*, 1082–1085.

(63) Holloway, J. L.; Gitlitz, M. H. *Can. J. Chem.* **1967**, *45*, 2659–2663.

(64) Richards, J. L.; Tarbell, D. S.; Hoffmeister, E. H. *Tetrahedron* **1968**, *24*, 6485–6493.

(65) Hadjikostas, C. C.; Katsoulos, G. A.; Shakhatareh, S. K. *Inorg. Chim. Acta* **1987**, *133*, 129–132.

(66) Lever, A. B. P. *Inorganic Electronic Spectroscopy*; Elsevier: Amsterdam, 1984.

(67) Pellicani, G. C.; Malavasi, W. D. D. *J. Inorg. Nucl. Chem.* **1975**, *37*, 477–481.

Table 1. Absorption Bands in the UV–Vis Electronic Spectra

compd	λ_{\max} (nm) (log ϵ)				
	band I	band II	band III	band IV	band V
[(DMDTM)AuCl ₃] ^a	218.4 (3.91)	244.0 (4.51)	284.3 (4.19)		409.8 (2.93)
[(DMDTM)AuBr ₃] ^a	217.9 (3.87)	240.3 (4.03)	280.8 (3.33)		407.8 (2.87)
[(DMDTM)AuCl] ^a	216.8 (3.97)	249.7 (4.00)	274.7 (4.04)	307.2 (3.37)	
[(DMDTM)AuBr] ^a	217.1 (3.99)	246.3 (3.89)	271.8 (4.21)	305.9 (3.22)	
[(ESDT)AuCl ₂] ^b	232.1 (3.87)	267.2 (4.52)	312.1 (4.05)		417.1 (3.01)
[(ESDT)AuBr ₂] ^b	236.2 (3.99)	261.3 (4.47)	310.4 (4.02)		415.2 (3.18)

^a Performed in CH₃CN in the range 210–900 nm. ^b Performed in CH₃OH in the range 210–900 nm.

Bands II and III show large molar extinction coefficients (ϵ) and correspond to intraligand $\pi^* \leftarrow \pi$ transitions mainly located in the –NCS and –CSS moieties, respectively.^{42,43} The former band is usually dependent on the nature of the alkyl moieties bound to the nitrogen atom⁶⁸ and, slightly, on the nature of the halogen atom.⁴³ On passage from gold(I) to gold(III) derivatives of the same dithiocarbamate ligand, band II is shifted to higher energies (that is, lower wavelengths) with increased formal charge on the central atom.⁶⁹ Conversely, the position of band III is very often dependent on the nature of the central atom but not on the type of the rest of the ligand.^{40,56,68} In gold(III) derivatives this band is generally shifted to greater wavelengths as the empty d orbitals of the metal atom lower the π -bonding level(s) of the ligand.⁶⁹ On the contrary, d¹⁰ metals, such as gold(I), have only a slight effect on its position, leading to a small increase in the transition energies.⁶⁹

Band IV is recorded only for gold(I) derivatives and is commonly assumed to be due to an intramolecular ligand-to-metal charge-transfer transition $\text{Au}(p) \leftarrow \text{S}(p)$.^{70,71}

At around 340 nm a low-intensity band should be recorded, corresponding to an intraligand $\pi^* \leftarrow n$ transition, where n is the in-plane nonbonding sulfur orbital;⁷² anyway, this band is not always detected due to the overlap of the close more intense bands.

In the gold(III) square-planar complexes, the d metal orbitals are split up in the following order of decreasing energy: $d_{x^2-y^2} > d_{xy} > d_{xz}, d_{yz} > d_z^2$. In the 6p shell, p_x and p_y are destabilized since they point directly toward the ligands, p_z remaining unaffected and, hence, most stable.^{39,73,74} On the basis of these considerations, all the gold(III) complexes give rise to a characteristic spectrum at the low-energy side of the main charge-transfer edge. The weakest band (band V) can be attributed to $d \leftarrow d$ metal orbitals transitions, and its position and intensity is clearly indicative of a square-planar environment for the metal in the investigated complexes. In particular, this broad band can be

(68) Katsoulos, G. A.; Tsipis, C. A. *Inorg. Chim. Acta* **1984**, *84*, 89–94.

(69) Nikolov, G. S.; Jordanov, N.; Havezov, I. *J. Inorg. Nucl. Chem.* **1971**, *33*, 1055–1065.

(70) Brown, D. H.; McKinlay, G.; Smith, W. E. *J. Chem. Soc., Dalton Trans.* **1977**, 1874–1879.

(71) Jiang, Y.; Alvarez, S.; Hoffmann, R. *Inorg. Chem.* **1985**, *24*, 749–757.

(72) Lee, A. W. M.; Chan, W. H.; Ho, M. F. *Anal. Chim. Acta* **1991**, 443–445.

(73) Gangopadhyay, A. K.; Chakrovarty, A. *J. Chem. Phys.* **1961**, *35*, 2206–2209.

(74) Chatt, J.; Gamlen, G. A.; Orgel, L. E. *J. Chem. Soc.* **1958**, 486–489.

Table 2. Thermogravimetric (TG) and Differential Scanning Calorimetric (DSC) Data

compd	Step	wt loss (%)		DSC: peak temp (°C) (process ^a)
		found	calcd	
[(DMDT)AuCl ₂]	I	33.97	34.28	254.8/327.4 (endo)
	II	49.22	49.25	538.2 (exo)
[(DMDT)AuBr ₂]	I	46.02	46.53	263.8/317.2 (endo)
	II	58.86	58.70	567.1 (exo)
[(DMDTM)AuCl ₃]	I	50.89	51.43	89.1/137.7/303.0 (endo)
	II	55.59	55.09	531.9 (exo)
[(DMDTM)AuBr ₃]	I	63.17	62.76	108.2/145.0/310.2 (endo)
	II	66.18	65.56	537.8 (exo)
[(DMDTM)AuCl]	I	29.81	?	152.7/183.4 (endo)
	II	46.27	46.43	331.0/475.2 (exo)
[(DMDTM)AuBr]	I	26.20	?	152.0/188.7 (endo)
	II	52.91	52.21	316.0/485.8 (exo)
[(ESDT)AuCl ₂]	I	43.92	44.57	192.1 (endo)
	II	57.65	57.20	498.8 (exo)
[(ESDT)AuBr ₂]	I	53.08	53.65	240.3 (endo)
	II	62.79	64.13	498.9 (exo)
[(ESDT)Au] ₂	I	34.17	34.48	268.7 (endo)
	II	48.94	49.40	503.6 (exo)

^a Endo/exo = endothermic/exothermic process.

assigned to ${}^1A_{2g} \leftarrow {}^1A_{1g}$ and ${}^1E_g \leftarrow {}^1A_{1g}$ transitions (spin allowed but symmetry forbidden) corresponding to the $d_{x^2-y^2} \leftarrow d_{xy}$ and $d_{x^2-y^2} \leftarrow d_{xz, yz}$ transitions, respectively.^{39,66,75} Anyway, the assignment of this band is still in debate as other authors have sometimes ascribed it to an intramolecular metal-to-ligand charge transfer from the d orbitals of the metal to the π^* system of the ligands.^{65,76}

Thermal Studies. The thermal behavior of the synthesized complexes has been studied by thermogravimetry (TG) and differential scanning calorimetry (DSC) techniques in a dynamic atmosphere of air, to establish the different decomposition processes and to confirm the proposed stoichiometry. The experimental data agree to a good extent with the data obtained by the other spectroscopic techniques, and the results of such analysis, summarized in Table 2, indicate a good correlation between calculated and found weight loss values for all the investigated compounds.

As regards DMDT and ESDT derivatives, the thermal degradation occurs in two successive well-defined steps. The first TG step corresponds to pyrolysis, decarboxylation (not for DMDT derivatives), and reductive elimination Au(III) \rightarrow Au(I), thus leading to [Au(SCN)] as the residue, a commonly discovered intermediate in the thermal decom-

(75) Clark, R. J. H.; Turtle, P. C. *J. Chem. Soc., Dalton Trans.* **1977**, 2142–2148.

(76) Franchini, G. C.; Giusti, A.; Preti, C.; Tosi, L.; Zanini, P. *Polyhedron* **1985**, *4*, 1553–1558.

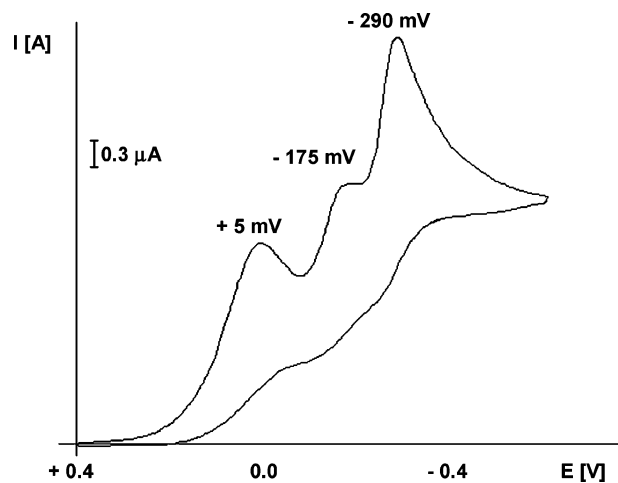


Figure 6. Cyclic voltammogram of [(DMDT)AuCl₂].

Table 3. Peak Potential Values (vs SCE) for the Reduction of the Present Gold(III) Complexes in Acetonitrile

compd	E_p (V)		
[(DMDT)AuCl ₂]	+0.005	-0.175	-0.290
[(DMDT)AuBr ₂]	+0.095	-0.073	-0.245
[(ESDT)AuCl ₂]	+0.038	-0.084	-0.195
[(ESDT)AuBr ₂]	+0.125	-0.058	-0.155

position of metal dithiocarbamates.^{77,78} A very intense effect is recorded at higher temperature, which corresponds to removal of the remaining ligand atoms, complete degradation leading to metallic gold.^{41,42,56} The formation of metallic gold as the final residue is confirmed by the presence of an endothermic DSC peak at 1066 °C due to the metallic gold melting.

For DMDTM gold derivatives too, thermal decomposition takes place in two different steps. For [(DMDTM)AuX₃] (X = Cl, Br) complexes, the first TG step corresponds to a reductive elimination process that leads to gold(I) sulfide as intermediate.⁷⁸ Conversely, [(DMDTM)AuX] (X = Cl, Br) complexes undergo a pyrolytic process whose intermediate decomposition product could not be undoubtedly established. Anyway, both gold(III) and gold(I) complexes experience pyrolytic processes that lead to the formation of metallic gold as the final residue, with experimental weight losses in good agreement with values calculated on the basis of the corresponding proposed stoichiometry.

Electrochemical Studies. The inherent electrochemical properties of the DMDT and ESDT gold(III) derivatives in acetonitrile have been studied through cyclic voltammetry soon after dissolution; since the redox transitions are chemically irreversible (see below), potentials can only be given as peak potentials (E_p , Table 3). As exemplified in Figure 6, which shows the cyclic voltammetric behavior of the compound [(DMDT)AuCl₂], it is apparent that the investigated complex undergoes two irreversible reduction processes

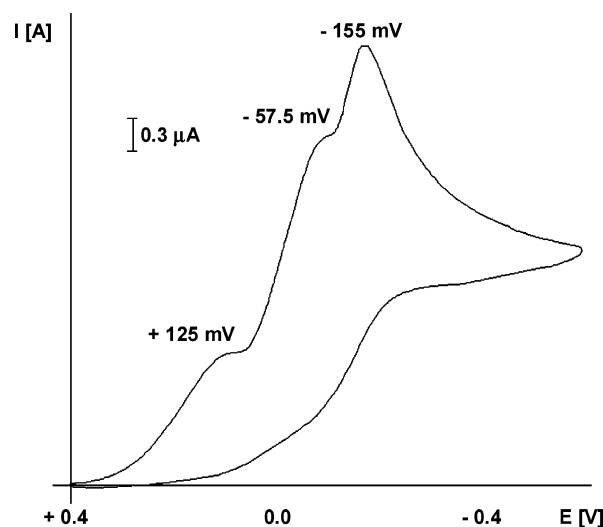


Figure 7. Cyclic voltammogram of [(ESDT)AuBr₂].

at +5.0 and -290.0 mV, respectively, which, in controlled-potential coulometry, involve one electron/molecule each. Thus, the gold(III) compound reduction proceeds through two separated Au(III)/Au(II) and Au(II)/Au(I) steps, the former probably leading to the formation of a dimeric gold(II) species with bridging chlorine atoms.⁷⁹ Exhaustive electrolysis at the second process leads to the precipitation of a solid residue, insoluble in acetonitrile, whose spectroscopic characterization is fully consistent with the gold(I) binuclear species [(DMDT)Au]₂.²⁴ An intermediate irreversible reduction process occurs at -175 mV involving 0.5 electron/molecule; this is probably due to the formation of a labile reduction intermediate or a mixed Au(II)/Au(I) derivative.

A similar behavior has been also observed for the analogous bromo-derivative [(DMDT)AuBr₂] and for the complexes of the type [(ESDT)AuX₂] (X = Cl, Br); in Figure 7, the cyclic voltammogram of [(ESDT)AuBr₂] is reported as example. As shown, the investigated complex undergoes three irreversible reduction processes at +125.0, -57.5, and -155.0 mV, respectively, but it was not possible to correctly establish, in controlled-potential coulometry, how many electrons the first two steps involve. On the other hand, it was calculated that the last process involves two electrons/molecule; even in this case, exhaustive electrolysis at the last process leads to the precipitation of a solid residue, insoluble in acetonitrile, whose spectroscopic characterization is completely consistent with the gold(I) binuclear species [(ESDT)Au]₂, which we have already synthesized and characterized. The two intermediate irreversible reduction processes, again, are probably due to the formation of labile reduction intermediates or mixed Au(II)/Au(I) derivatives.

For both [(DMDT)AuX₂]- and [(ESDT)AuX₂]-type complexes, reductions occur at potentials considerably below the typical value of the Au(III)/Au(I) couple known for the corresponding KAuX₄ (X = Cl, Br) halide precursors (E°

(77) Macias, B.; Criado, J. J.; Vaquero, M. V.; Villa, M. V. *Thermochim. Acta* **1993**, *223*, 213–221.

(78) Fernandez-Alba, A.; Perez-Alvarez, I. J.; Martinez-Vidal, J. L.; Gonzalez-Pradas, E. *Thermochim. Acta* **1992**, *211*, 271–277.

(79) Antonova, L. V.; Busygina, T. E.; Polovnyak, V. K.; Usachev, A. E. *Russ. J. Gen. Chem.* **1997**, *67*, 529–532.

Table 4. Evaluation of in Vitro Cytotoxic Activity [$IC_{50} \pm SD$ (μM)] of the Investigated Gold(III) Complexes toward Established Human Tumor Cell Lines by MTT Testing after 24 h^a

cell line	compd				
	[(DMDT)AuCl ₂]	[(DMDT)AuBr ₂]	[(ESDT)AuCl ₂]	[(ESDT)AuBr ₂]	cisplatin
HeLa	2.10 ± 0.01	3.50 ± 0.01	8.2 ± 0.2	7.6 ± 0.2	15.6 ± 0.4
HL60	(0.80 ± 0.01) × 10 ⁻²	(0.70 ± 0.01) × 10 ⁻²	0.43 ± 0.09	0.14 ± 0.02	25.6 ± 0.3
Daudi	(0.10 ± 0.01) × 10 ⁻²	(0.10 ± 0.01) × 10 ⁻²	4.65 ± 0.09	5.8 ± 0.2	95 ± 1
MeWo	2.0 ± 0.3	(0.10 ± 0.01) × 10 ⁻²	12.5 ± 0.9	10.0 ± 0.9	48 ± 2
LoVo	(2.40 ± 0.04) × 10 ⁻²	3.8 ± 0.1	7.6 ± 0.2	7.9 ± 0.1	56 ± 2
A549	(0.35 ± 0.01) × 10 ⁻²	0.41 ± 0.03	4.73 ± 0.04	9.6 ± 0.2	35 ± 1

^a IC_{50} values were calculated by probit analysis ($P < 0.05$, χ^2 test).

= ~1.29 V).⁸⁰ Indeed, coordination by dithiocarbamates induces a large stabilization of the +3 oxidation state of the gold center, owing to the electron-donating ability and the chelate effect of the dithiocarbamate moiety.¹⁵ Noticeably, the ESDT ligand induces a lower stabilization of gold(III) compared to DMDT ligand.

In Vitro Cytotoxic Activity. Before use, all the tested compounds were dissolved in DMSO just before the experiments; calculated amounts of drug solution were then added to phosphate buffered saline (0.138 M NaCl, 0.0027 M KCl, phosphate buffer pH = 7.4) solution or to the growth medium containing cells, to a final solvent concentration of 0.5%, which had no discernible effect on cell killing. All the tested complexes have been proved, by ¹H NMR studies, to be stable in DMSO over 48 h.

First, the cytotoxic activity of all the investigated gold(I) and gold(III) dithiocarbamate derivatives and dithiocarbamate ligands has been evaluated, for a preliminary screening, toward HL60 cells, as they are highly sensitive to any cytotoxic agent (see Supporting Information). With analysis of the percentage of HL60 cells vitality with respect to control (cisplatin) upon 24 h of incubation of increasing amounts of the tested gold complexes, it is apparent that DMDTM gold derivatives show no or slight cytotoxic activity, whereas, for all the DMDT and ESDT gold(III) derivatives, cytotoxicity values are much higher than the reference drug even at low concentrations. Remarkably, DMDT gold(III) complexes are highly cytotoxic whereas the free DMDTNa is not, implying that biological activity is to be essentially ascribed to the presence of the gold(III) metal center. The binuclear gold(I) complex [(ESDT)Au]₂ produces a smaller inhibition of cell growth in comparison to the gold(III) analogues, even if its antiproliferative activity remains higher or, at least, comparable with that of cisplatin.

On the basis of these preliminary results, the four complexes [(DMDT)AuX₂] and [(ESDT)AuX₂] (X = Cl, Br) have been submitted to further in vitro cytotoxicity tests. A first set of experiments has been performed on a panel of six human tumor cell lines to establish a cancer-type-specific antitumor action. This panel includes HeLa (human squamous cervical adenocarcinoma), HL60 (human leukemic promyelocytes), Daudi (human Burkitt's lymphoma), MeWo (human malignant melanoma), LoVo (human colon adenocarcinoma), and A549 (human nonsmall lung adenocarci-

noma) established cell lines grown in vitro. Cytotoxicity has been evaluated by means of MTT test; for comparison purpose, the cytotoxicity of cisplatin has been also evaluated under the same experimental conditions and the results have been summarized in terms of IC_{50} values in Table 4. It is apparent that all the investigated gold(III) compounds exhibit relevant cytotoxic activities toward all the tested cell lines, in particular on the lymphoproliferative-type tumor cells HL60 and Daudi, which have been proved to be more drug sensitive than solid tumor cell lines. Remarkably, they appear to be much more potent than cisplatin even at nanomolar concentration, with IC_{50} values about 1- to 4-fold lower than that of the reference drug.

Data regarding their in vitro antiproliferative activity against colon and nonsmall cells lung adenocarcinoma cell lines, which are notoriously not very sensitive to cisplatin,⁸¹ are extremely interesting because these new gold(III) complexes seem to be cytotoxic also against tumor cell lines resistant to cisplatin, overcoming their intrinsic resistance.

Data reported in Table 4 refers to in vitro cytotoxicity evaluated after a 24 h contact between the tumor cells and the gold(III) compounds. Moreover, drug profiles have been also evaluated after 48 and 72 h; for example, in Table 5 IC_{50} values, obtained toward human ovarian carcinoma 2008 cells after 24, 48, and 72 h of incubation, are reported. These data clearly show that the cell growth inhibitory effect of the investigated gold(III) compounds is not time-dependent; in fact, they exert their cytotoxic activity mainly within the first 24–48 h, and the IC_{50} values remains similar after 48 and 72 h. Conversely, the antiproliferative activity of cisplatin increases proportionally with time, its IC_{50} values being comparable to those of the gold(III) complexes generally after 72 h.

To assess the possible lack of cross-resistance with cisplatin, a second set of experiments has been performed, under the same experimental conditions above reported, on a panel of six human tumor cell lines sensitive and resistant to cisplatin: 2008/C13* (human ovarian carcinoma), A431/A431-R (human squamous cervix carcinoma), and U2OS/U2OS-R (human osteosarcoma) cells. Cytotoxic activity has been evaluated by means of MTT test; for comparison purpose, the cytotoxicity of cisplatin has been also evaluated under the same experimental conditions (Table 6). Cross-resistance profiles are evaluated by means of the resistance

(80) Koelle, U.; Laguna, A. *Inorg. Chim. Acta* **1999**, *290*, 44–50.

(81) Wang, X.; Zhang, Z.; Li, X. *Zhongguo Yaolixue Tongbao* **2002**, *18*, 144–148.

Table 5. Evaluation of in Vitro Cytotoxic Activity of the Investigated Gold(III) Complexes toward the 2008 Cell Line by MTT Testing with Time^a

compd	2008 cell line IC ₅₀ ± SD (μM)		
	24 h	48 h	72 h
[(DMDT)AuCl ₂]	(0.20 ± 0.01) × 10 ⁻²	(0.20 ± 0.01) × 10 ⁻²	(0.10 ± 0.01) × 10 ⁻²
[(DMDT)AuBr ₂]	30.1 ± 0.1	6.1 ± 0.1	5.1 ± 0.2
[(ESDT)AuCl ₂]	49.3 ± 0.1	4.9 ± 0.6	4.5 ± 0.3
[(ESDT)AuBr ₂]	16.5 ± 0.4	5.22 ± 0.1	4.5 ± 0.9
cisplatin	43.2 ± 0.4	30.3 ± 0.3	7.9 ± 0.4

^a IC₅₀ values were calculated by probit analysis ($P < 0.05$, χ^2 test).

Table 6. Evaluation of in Vitro Cytotoxic Activity [IC₅₀ ± SD (μM)] of the Investigated Gold(III) Complexes toward Established Cisplatin-Sensitive and -Resistant Human Tumor Cell Lines by MTT Testing after 24 h^a

compd	2008	C13*	RF
[(DMDT)AuCl ₂]	(0.20 ± 0.01) × 10 ⁻²	(0.10 ± 0.01) × 10 ⁻²	0.50
[(DMDT)AuBr ₂]	30.1 ± 0.1	21.8 ± 0.2	0.73
[(ESDT)AuCl ₂]	49.3 ± 0.1	23.8 ± 0.1	0.48
[(ESDT)AuBr ₂]	16.5 ± 0.4	(0.10 ± 0.01) × 10 ⁻²	0.6 × 10 ⁻⁴
cisplatin	43.2 ± 0.4	556 ± 3	12.86

compd	A431	A431-R	RF
[(DMDT)AuCl ₂]	(1.20 ± 0.01) × 10 ⁻²	(0.20 ± 0.01) × 10 ⁻³	0.017
[(DMDT)AuBr ₂]	1.8 ± 0.1	2.8 ± 0.2	1.56
[(ESDT)AuCl ₂]	0.29 ± 0.01	0.43 ± 0.03	1.48
[(ESDT)AuBr ₂]	(1.50 ± 0.01) × 10 ⁻²	(0.10 ± 0.01) × 10 ⁻²	0.06
cisplatin	77.4 ± 0.4	382 ± 3	4.93

compd	U2OS	U2OS-R	RF
[(DMDT)AuCl ₂]	4.8 ± 0.3	6.4 ± 0.1	1.33
[(DMDT)AuBr ₂]	18 ± 1	13 ± 1	0.72
[(ESDT)AuCl ₂]	5.8 ± 0.4	5.2 ± 0.2	0.88
[(ESDT)AuBr ₂]	0.49 ± 0.09	0.24 ± 0.09	0.49
cisplatin	35 ± 2	84 ± 3	2.37

^a IC₅₀ values were calculated by probit analysis ($P < 0.05$, χ^2 test).

factor (RF), which is defined as the ratio between IC₅₀ values calculated for cisplatin-resistant cell line and the sensitive parental cell line respectively (RF = IC₅₀-resistant/IC₅₀-sensitive). Remarkably, all the tested gold(III) complexes are much more cytotoxic than the reference drug on cisplatin-resistant cell lines, with activity levels comparable to those induced on the parental sensitive cell lines, ruling out the occurrence of cross-resistance phenomena.

Clonogenic Assays. To assess the capability for cell unlimited proliferation after drug exposure, we monitored the sustained proliferation of surviving cells by a clonogenic assay on the human squamous cervical adenocarcinoma HeLa cells; for comparison purpose, cisplatin was also evaluated under the same experimental conditions. More clonogenic tests have been also performed toward other cisplatin-sensitive and -resistant cell lines, such as 2008/C13* and A431/A431-R pairs, to verify the results previously observed (see Supporting Information). On the basis of this assay, all the tested complexes have been proved to be less active than cisplatin on sensitive cells but display, as expected, a significantly higher activity against the resistant parental cell lines. Compared to previously reported in vitro cytotoxicity data carried out toward the same cell lines, these results are quite surprising; in fact, cytotoxic activity obtained by means of MTT test showed that the investigated gold(III) complexes were much more active than cisplatin against all the cells

here examined. Anyway, it is worth reminding that those results were referred to acute short-term cytotoxicity, whereas clonogenic tests evaluate incidental damages eventually induced to the cell progeny. Thus, we could hypothesize that these gold(III) complexes are so highly cytotoxic that they cause an immediate aspecific damage to the cells, leading to their apoptosis, whereas nondamaged surviving cells can proliferate without inducing any damage to their progeny.

Final Remarks. Although none of the complexes here reported has been obtained in the crystalline state, and thus the structures cannot be undoubtedly proposed, the conclusions reached upon application of the spectroscopic techniques suggest that coordination of all the DMDT and ESDT gold(III) derivatives takes place in a near-square-planar geometry through the sulfur-donating atoms, the -NCSS group coordinating the metal center in a bidentate symmetrical mode and lying in the same plane.

As regards the gold(I) dithiocarbamate derivative [(ESDT)-Au]₂, each ESDT ligand binds the two metal centers in a bidentate symmetrical mode, thus leading to a binuclear cyclic complex exhibiting two linear S-Au-S bonds.

In the DMDTM gold(III) and gold(I) derivatives, the DMDTM ligand is linked to the metal ion through the thiocarbonyl sulfur atom, the remaining coordination position(s) being occupied by halogen atom(s); [(DMDTM)-AuCl₃] and [(DMDTM)AuBr₃] complexes are tetracoordinated in the usual square-planar geometry, whereas the gold(I) analogues exhibit a characteristic S-Au-X (X = Cl, Br) linear structure.

Among all the gold dithiocarbamate derivatives here reported, DMDT and ESDT gold(III) derivatives ([DMDT)-AuX₂] and [(ESDT)AuX₂], X = Cl, Br) have been proved to be much more cytotoxic in vitro than cisplatin even toward human tumor cell lines intrinsically resistant to cisplatin itself. Moreover, they appeared to be much more cytotoxic also on the cisplatin-resistant cell lines, with activity levels comparable to those on the corresponding cisplatin-sensitive cell lines, ruling out the occurrence of cross-resistance phenomena and supporting the hypothesis of a different antitumor activity mechanism of action.⁸²

Acknowledgment. The authors gratefully acknowledge partial financial support of this work by the Ministero dell'Università e della Ricerca Scientifica e Tecnologica

(82) Fregona, D.; Ronconi, L.; Marzano, C. Complessi ditiocarbammici di oro(III) e loro impiego come antitumorali. Italian Patent No. MI2003A000600, Mar 26, 2003.

Gold Dithiocarbamate Derivatives

(pharmacological and diagnostic properties of metal complexes).

Supporting Information Available: Drug sensitivity profiles of the HL60 cell line, cross-resistance profiles, and clonal growth

profiles. This material is available free of charge via the Internet at <http://pubs.acs.org>.

IC048260V